Fluorescent Actin Analogs with a High Affinity for Profilin In Vitro Exhibit an Enhanced Gradient of Assembly in Living Cells

Kenneth A. Giuliano and D. Lansing Taylor

Center for Light Microscope Imaging and Biotechnology and Department of Biological Sciences, Carnegie Mellon University, Pittsburgh, Pennsylvania 15213

Abstract. Constitutive centripetal transport of the actin-based cytoskeleton has been detected in cells spreading on a substrate, locomoting fibroblasts and keratocytes, and non-locomoting serum-deprived fibroblasts. These results suggest a gradient of actin assembly, highest in the cortex at the cytoplasm-membrane interface and lowest in the non-cortical perinuclear cytoplasm. We predicted that such a gradient would be maintained in part by phosphoinositide-regulated actin binding proteins because the intracellular free Ca^{2+} and pH are low and spatially constant in serum-deprived cells. The cytoplasm-membrane interface presents one surface where the assembly of actin is differentially regulated relative to the non-cortical cytoplasm. Several models, based on in vitro biochemistry, propose that phosphoinositide-regulated actin binding proteins are involved in local actin assembly. To test these models in living cells using imaging techniques, we prepared a new fluorescent analog of actin that bound profilin, a protein that interacts with phosphoinositides and actin-monomers in a mutually exclusive manner, with an order of magnitude greater affinity (K_d = 3.6 μM) than cys-374–labeled actin (K_d > 30 μM), yet retained the ability to inhibit DNase I. Hence, we were able to directly compare the distribution and activity of a biochemical mutant of actin with an analog possessing closer to wild-type activity. Three-dimensional fluorescence microscopy of the fluorescent analog of actin with a high affinity for profilin revealed that it incorporated into cortical cytoplasmic fibers and was also distributed diffusely in the non-cortical cytoplasm consistent with a bias of actin assembly near the surface of the cell. Fluorescence ratio imaging revealed that serum-deprived and migrating fibroblasts concentrated the new actin analog into fibers up to four-fold in the periphery and leading edge of these cells, respectively, relative to a soluble fluorescent dextran volume marker, consistent with the formation of a gradient of actin filament density relative to cell volume. Comparison of these gradients in the same living cell using analogs of actin with high and low affinities for profilin demonstrated that increased profilin binding enhanced the gradient. Profilin and related proteins may therefore function in part to bias the assembly of actin at the membrane–cytoplasm interface.

LOCOMOTION and cytokinesis require the precisely orchestrated activity of actin assembly, myosin motor proteins, actin filament severing, crosslinking, and bundling proteins, and a family of actin-monomer-binding proteins (Stossel, 1989; Hartwig and Kwiatkowski, 1991). Maintaining the precise distribution of ions, metabolites, macromolecules, and organelles in time and space within the living cell must also be considered a much more subtle expression of intracellular motility. A characteristic of the cytoplasm of motile and nonmotile cells is the centripetal transport of the actin-based cytoskeleton (Giuliano and Taylor, 1990; Heath and Holifield, 1991; Conrad et al., 1993). It has been suggested to involve an integrated cycle of actin assembly and crosslinking into a meshwork near the cytoplasm–membrane interface (Wang, 1985; Fisher et al., 1988; Forscher and Smith, 1988), transport of the meshwork away from the edge of the cell (McKenna et al., 1989; Giuliano and Taylor, 1990; Conrad et al., 1993), and disassembly of the meshwork in the perinuclear region with contraction in motile cells (Dunn, 1980; Kolega and Taylor, 1993) or without contraction in nonmotile cells (Giuliano and Taylor, 1990; Kolega and Taylor, 1993). One general description of this cycle has been called cortical flow (Bray and White, 1988). It is therefore essential that we map the dynamic distribution of actin in its many states in both locomoting and stationary, yet biologically active cells.

Address all correspondence to K. A. Giuliano, Center for Light Microscope Imaging and Biotechnology, Carnegie Mellon University, 4400 Fifth Avenue, Pittsburgh, PA 15213.

Implicit in the description of cortical flow is the existence of a gradient of actin assembly that we predict would be maximal at the cytoplasm-membrane interface where actin subunits preferentially incorporate into the meshwork of actin-based cytoskeleton (Wang, 1985; Fisher et al., 1988; Forscher and Smith, 1988; Okabe and Hirokawa, 1989; Symons and Mitchison, 1991) and into specializations of the actin-based cytoskeleton-like stress fibers (Wang, 1984; Giuliano and Taylor, 1990) and actin arcs (DeBiasio et al., 1988; Heath and Holifield, 1991). It follows that actin disassembly might dominate in the perinuclear region where stress fibers constitutively disassemble in serum-deprived cells (Giuliano and Taylor, 1990) and where diffuse actin accumulates upon the dispersion of actin arcs in spreading cells (Wang, 1984; DeBiasio et al., 1988). Furthermore, optimal incorporation of actin into the cytoskeleton is likely to be predicated on the interaction of actin with a host of precisely localized or regulated actin binding proteins (Stossel, 1989, 1990).

Fluorescent analogs of actin have been prepared with sulfhydryl- and amino-reactive dyes and used to map the dynamics of the whole actin population in living cells, while analyzing a subset of actin with photobleaching (Taylor and Wang, 1978; Wang and Taylor, 1980; Kreis et al., 1982; Amato and Taylor, 1986) or with a photo-activated fluorescent dye (Theriot and Mitchison, 1991). Fluorescent actin analogs exhibit incorporation into stress fibers, an immobile fraction, and hindered diffusion in living cells (Kreis et al., 1982; Luby-Phelps et al., 1985; Wang, 1985; Amato and Taylor, 1986; Theriot and Mitchison, 1991) despite nearly all of them being labeled at cys-374, a site known to be in the region important for the interaction of actin monomers during polymerization and for the binding of several actin-binding proteins (Kabsch and Vandekerckhove, 1992). For example, the binding of actin monomers by profilin is dramatically decreased when cys-374 of actin is chemically modified (Malm, 1984) or mutated (Aspenstrom et al., 1993). It would therefore be useful to prepare fluorescent analogs of actin with a higher affinity for profilin and to compare the incorporation of the new actin analogs with the traditional cys-374–labeled analogs into the actin-based cytoskeleton in the same cell. It is essential to do comparisons of this sort in the same cell because the biological heterogeneity between cells may preclude meaningful conclusions when comparing results of experiments in separate cells unless statistical analyses are performed on very large data sets, a situation that is difficult to create in microscope studies of living cells. Examples of this heterogeneity become evident in describing the dynamics of the actin-based cytoskeleton (Giuliano and Taylor, 1990), effector-induced changes in intracellular pH (Bright et al., 1989) and free Ca^{2+} (Byron and Villereal, 1989), and calmodulin activation (Hahn et al., 1992; Gough and Taylor, 1993) in single living cells.

Materials and Methods

Protein Purification

Bovine spleen profilactin was purified at 4°C as follows: spleen obtained from a local slaughterhouse was cleaned, chopped, quick frozen in liquid nitrogen, and stored at −70°C until needed. Partially thawed tissue weighing 250 g was homogenized in 2.5 volumes of Buffer B (10 mM Tris-HCl, 50 mM NaCl, 1 mM NaN_3, 0.5 mM DTT, pH 7.5 at 23°C) in a blender using 20-s bursts every minute for 3 min. The homogenate was centrifuged for 30 min at 20,000 *g*. The supernatant was centrifuged again for 1 h at 100,000 *g*. The high speed supernatant was filtered through glass wool and loaded onto a DE-52 column (5 × 19 cm; two tissue volumes) equilibrated with Buffer B. Washing the column with Buffer B eluted free profilin and pigmented material that caused fouling of the subsequent affinity column if it was not removed beforehand. Profilactin was eluted by washing with one column bed volume of Buffer B containing 0.6 M KCl. The cloudy eluate was centrifuged for 1 h at 100,000 *g* and loaded onto a poly-L-proline Sepharose column (2.5 × 15 cm) equilibrated with Buffer B. After washing the column with Buffer B, profilactin was eluted as described by Rozycki et al. (1991) with Buffer B minus DTT, but containing 40% (vol/vol) DMSO. The eluate was immediately dialyzed against saturated ammonium sulfate (pH 7) to remove the DMSO and precipitate the 35–50 mg of profilactin obtained with this procedure.

We prepared spleen actin and profilin from profilactin by modifying a previous procedure (Malm et al., 1983). Profilactin, stored at 4°C in ammonium sulfate, was centrifuged for 30 min at 27,000 *g*. The pellet was dissolved in a minimal amount of Bicine Buffer A (2 mM Bicine, 0.2 mM Na_2ATP, 0.2 mM $CaCl_2$, 50 mM KCl, 0.5 mM DTT, pH 8.3 at 23°C) and dialyzed against the same. We added an equal volume of Actin Paracrystal Buffer (2 M potassium phosphate, 4 mM Na_2ATP, 6 mM $MgCl_2$, 2 mM DTT, pH 7.6 at 23°C) to the dialysate and gently rocked the solution at room temperature for 1 h. The actin paracrystals that formed were collected by centrifugation for 30 min at 100,000 *g*. The actin was washed by suspending the paracrystals in Actin Paracrystal Buffer that had been diluted 1:2 and centrifuging as above. The supernatants were pooled and used for the preparation of profilin as described below. The pellet containing actin paracrystals was homogenized in Buffer A (2 mM Tris-HCl, 0.2 mM Na_2ATP, 0.2 mM $CaCl_2$, 1 mM NaN_3, 0.5 mM DTT, pH 8.0 at 23°C) and dialyzed against the same buffer. The dialysate was centrifuged for 2 h at 100,000 *g* and the supernatant loaded onto a Sephadex G-150 gel filtration column (2.5 × 95 cm) equilibrated with Buffer A. The monomeric actin eluting from the column was concentrated using 25,000 M_r cutoff ultrafiltration cones (Amicon Corporation, Beverly, MA), polymerized in 100 mM KCl and 2 mM $MgCl_2$, pelleted, and finally disassembled by dialysis against Buffer A minus NaN_3 in a Collodion 25,000 M_r cutoff bag (Schleicher and Schuell, Keene, NH). Small aliquots of monomeric actin were quick frozen in liquid nitrogen and stored at −70°C.

We purified profilin from the supernatants obtained from the preparation of spleen actin by dialyzing them against Buffer B containing 2 M urea followed by chromatography on a 5 ml column of DE-52 equilibrated with the same buffer. Profilin found in the flow-through was dialyzed against saturated ammonium sulfate and stored at 4°C as a precipitate.

Nomenclature of Fluorescently Labeled Actins

Labeled actins were distinguished from each other using a four letter abbreviation (i.e., sAmR-actin). The first letter signifies the source of the actin, either rabbit skeletal muscle (m) or bovine spleen (s). The next two letters describe the site of actin labeling, an acetamido (Ac) linkage to cys-374 or an amido (Am) linkage to a free amino group. The fourth letter stands for either carboxyfluorescein (F) or carboxytetramethylrhodamine (R).

Preparation of Cys-374-Modified Fluorescent Actin Analogs

Rabbit skeletal muscle actin was prepared according to Pardee and Spudich (1982). We labeled skeletal muscle and spleen actin at residue cys-374 with either carboxytetramethylrhodamine-5-(and -6)-iodoacetamide or 5-iodoacetamidocarboxyfluorescein (Molecular Probes, Inc., Eugene, OR) as described by Wang and Taylor (1980).

Preparation of Fluorescent Analogs of Actin with an Increased Affinity for Profilin

Amidocarboxytetramethylrhodamine (sAmR) and amidocarboxyfluorescein (sAmF) actins were prepared by reacting profilactin (5–7 mg/ml) with a 10-fold molar excess of the succinimidyl ester of 5- (and -6)-carboxyfluorescein or 5- (and -6)-carboxytetramethylrhodamine (Molecular Probes, Inc.) for 1 h at room temperature in Bicine Buffer A. Labeled actin was then purified from the complex by forming actin paracrystals as described above.

Measurement of the Dissociation Constant for Reconstituted Profilactin Complexes

The apparent dissociation constants (K_d) of reconstituted profilactin complexes were measured at 4°C in Buffer A using the sedimentation equilibrium method described by Clarke and Howlett (1979). Briefly, 100-μl samples containing 5 μM actin or actin analog, 5 μM profilin, and 5 mg/ml dextran (M_r 40,000) to stabilize the gradients were centrifuged at 30,300 *g* until sedimentation equilibrium was attained (20–22 h). The upper 40 μl of each sample was then carefully removed, diluted with 210 μl Buffer A, and assayed for actin concentration using spectrofluorimetry and the DNase I inhibition assay (Heacock and Bamburg, 1983). The fraction of actin left in the upper 40% of the tube after sedimentation in the presence or absence of profilin was used to calculate the K_d (Clarke and Howlett, 1979).

Cell Culture

For some experiments we prepared serum-deprived Swiss 3T3 fibroblasts as described (Giuliano and Taylor, 1990). Other experiments required migrating fibroblasts undergoing different phases of the wound healing response. A wound was introduced in a stable monolayer of Swiss 3T3 fibroblasts (DeBiasio et al., 1988; Conrad et al., 1993) and the cells at the edge of the wound were observed during the lamellar contraction stage of the process (3–6 h after wounding). We also devised a modified wound healing protocol to generate large numbers of fully locomoting fibroblasts. The day before an experiment, 75 μl of a suspension of cells (50,000 cells/ml) was spotted in the center of a dry 40-mm coverglass in a petri dish. After an hour in the incubator most of the cells had attached to the glass. 5 ml of culture medium was gently added and the cells were allowed to spread overnight into a nearly confluent monolayer. To initiate cell polarization and locomotion, half of the spotted cells were scraped away with a razor blade leaving a semi-circle of cells with a sharp edge. A synchronized line of migrating cells with few cell–cell contacts developed 2.5–4 h after wounding.

Microinjection and Microscopy

Approximately 5–10% of a cell volume (Amato et al., 1983) of a stock solution containing a mixture of two distinctly labeled actin analogs at 3–5 mg/ml and 1 mg/ml Cascade Blue dextran (M_r 10,000; Molecular Probes, Inc.) purified according to Pagliaro and Taylor (1988) in Buffer A was microinjected into fibroblasts. Because the extent of labeling varied, the amount of actin analogs in the injection solution was adjusted so that the concentration of each labeled species was approximately equal. Injected cells were allowed to recover for at least 1 h, then placed in a chamber on a temperature-controlled stage and either imaged with a multimode microscope (Biological Detection Systems, Inc., Pittsburgh, PA) as described by Giuliano et al. (1990) using a 576 × 384 Thompson chip cooled CCD camera (Photometrics Ltd., Tucson, AZ) or used for fluorescence recovery after photobleaching experiments (Pagliaro and Taylor, 1988). For fluorescence recovery experiments we used a 40× Plan-Neofluar objective (NA 0.9). Perinuclear and peripheral data were collected by bleaching a 5.5-μm spot within 10 μm of the nucleus and cell edge, respectively. We performed ratio imaging according to DeBiasio et al. (1988) with a 63× Plan-Neofluar (NA 1.25) or a 100× Plan objective (NA 1.30) and a cooled CCD camera. Unless otherwise noted, the numerator for our ratio measurements was the image obtained of the fluorescent actin analog, representing the distribution of total actin in the cytoplasm and included both assembled and unassembled actin species. The denominator was the fluorescence of Cascade Blue dextran and represented the volume of the cytoplasm accessible to particles of the same molecular dimensions (Luby-Phelps et al., 1985; DeBiasio et al., 1988). Consequently, the ratio was a measure of the concentration of actin (in all its forms) relative to the concentration of the freely diffusible Cascade Blue dextran. Within the volume accessible to actin, the ratio was always non-zero, as both actin and the volume marker were present. The ratio was zero only where there was no detectable fluorescent actin analog. When the fluorescent actin analog was detected, the ratio was minimal where there was no local enrichment of actin relative to the volume marker, i.e., a minimal level of actin assembly. We operationally defined the regions of cells with the highest ratio of actin filament density to dextran as being the regions of highest assembly of actin.

Three-dimensional fluorescence microscopy was performed by acquiring a through focus series of 30 images for each cell microinjected with the fluorescent analog of actin. The nearest neighbor algorithm was used to correct for out-of-focus fluorescence (Biological Detection Systems, Inc.) as described previously (Kolega and Taylor, 1993).

Results

Cys-374–labeled Actin Did Not Exhibit a Gradient of Filament Density Relative to Cell Volume in Live Serum-deprived Cells

Fig. 1 *A* depicts schematically our previous results showing that stress fibers constitutively form in the periphery of serum-deprived cells and are transported to the perinuclear region where they disappear without shortening (Giuliano and Taylor, 1990). Based on these observations and other results showing that stress fibers are localized in the cortex of these cells (Kolega and Taylor, 1993), we predicted that actin filament density relative to cell volume would be greatest in the cell periphery where the cell surface/volume ratio is maximal, and lowest in the thick perinuclear region where the cell surface/volume ratio is minimal. To test the prediction we microinjected cells with a fluorescent analog of cys-374–labeled actin (Fig. 1 *B*), a second analog of actin labeled distinctly (see below), and a cell volume marker (Fig. 1 *C*) that served to map the cytoplasmic volume with an intensity proportional to the pathlength and accessible volume of the cell (DeBiasio et al., 1988). The ratio image of mAcR-actin/volume marker (Fig. 1 *D*) did not exhibit a gradient of filament density relative to cell volume (see also Fig. 3 *D*, *dotted line*) suggesting that mAcR-actin distributed much like the dextran volume marker (Fig. 1 *C*) except that it was readily incorporated into stress fibers (Fig. 1 *B*). If profilin and other proteins are involved in biasing actin assembly near the plasma membrane (Lassing and Lindberg, 1988; Hartwig et al., 1989; Stosel, 1989), then it is not surprising that cys-374–labeled actin did not exhibit a gradient of filament density relative to cell volume because cys-374 is located in a region of the actin molecule important for actin-profilin interactions (Malm, 1984). We therefore prepared a new fluorescent analog of actin with a higher affinity for profilin than cys-374–labeled actin analogs.

A New Fluorescent Actin Analog Has a Higher Affinity for Profilin than the Traditional, Biochemically Mutated, Cys-374–labeled Analog while Retaining Its Ability to Inhibit DNase I

We prepared a new fluorescent actin analog by labeling free amino groups of actin while it was complexed with profilin using the succinimidyl ester of either carboxyfluorescein or carboxytetramethylrhodamine. The assembly properties of the new actin analog were similar to native actin since the critical concentration was 0.1 μM in 2 mM $MgCl_2$ and 100 mM KCl, a value equal to that of unlabeled spleen actin (Larsson and Lindberg, 1988). In addition, the fluorescence spectrum of the new actin analog showed no change upon assembly to the filamentous form. The dye/protein ratio for all of the actin analogs was in the range of 0.3–0.8.

We tested the ability of all of our actin analogs to recombine with unlabeled profilin under low salt conditions using sedimentation equilibrium (Clarke and Howlett, 1979). The apparent dissociation constant (K_d) value we measured for unlabeled spleen profilactin (Fig. 2) agreed well with the K_d

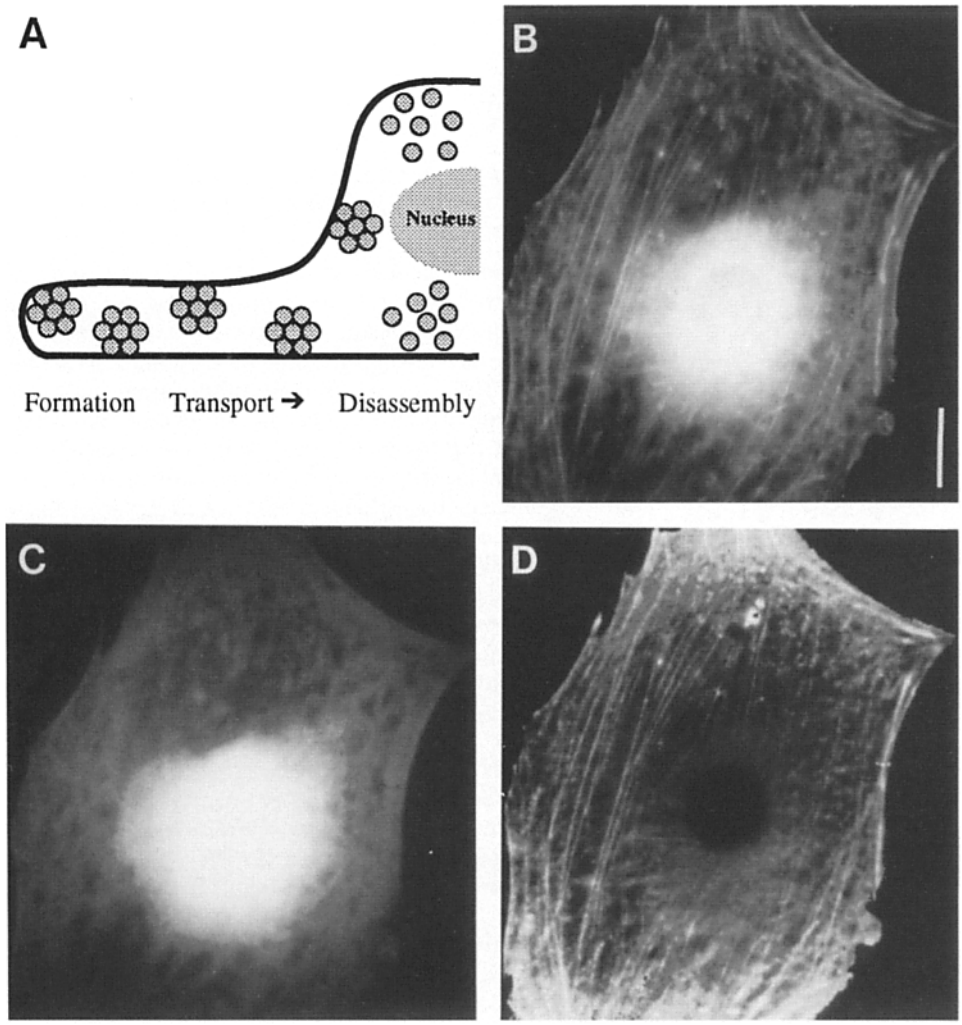

Figure 1. Cys-374–modified actin did not exhibit a gradient of filament density relative to cell volume across the width of a serum-deprived fibroblast. (*A*) The dynamics of stress fibers, shown here schematically in cross section as bundles of actin filaments, suggest that there is a net assembly of actin in the thin peripheral region of the cell where stress fibers constitutively form, and a net disassembly of actin in the thick perinuclear region where stress fibers constitutively disappear (Giuliano and Taylor, 1990). (*B*) A serum-deprived cell was microinjected with three distinct fluorescent probes to quantify their relative distributions. Shown here is the fluorescence image of mAcR-actin. (*C*) Fluorescence image of a cell volume marker (Cascade Blue dextran) in the same cell. (*D*) Ratio image of mAcR-actin/volume marker (*B*/*C*). Although mAcR-actin was incorporated into stress fibers, it did not exhibit a gradient of filament density relative to cell volume (see scan line data in Fig. 3). These patterns of actin distribution were consistent in the >100 cells observed. Bar, 10 μm.

of 0.4 μM measured under actin assembly conditions (50 mM KCl + 1 mM $MgCl_2$) for the same complex using viscometry (Larsson and Lindberg, 1988). Nonmuscle actin labeled as a complex with profilin recombined with profilin with an order of magnitude greater affinity than other analogs of actin labeled at cys-374 (Fig. 2) consistent with the finding of Malm (1984) and Aspenström et al. (1993) who showed that profilin binding is dramatically decreased when cys-374 of actin is chemically modified or mutated. These data suggest that the affinity of actin analogs for profilin depended only on the site of actin labeling, not the source of the actin (skeletal vs. nonmuscle) or the fluorescent dye used to label the actin (carboxyfluorescein vs. carboxytetramethylrhodamine). The affinity of our new actin analogs (sAmR-actin and sAmF-actin) for profilin was less than the affinity of unlabeled nonmuscle actin for profilin. We have been unable to find conditions that produce labeled actin with the maximal affinity for profilin. However, we have two actin analogs: one a severe biochemical "mutant" that has a low affinity for profilin and another that exhibits a ten-fold increase in affinity for profilin.

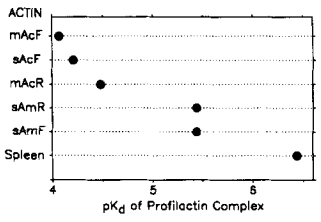

Figure 2. Apparent dissociation constants of profilactin complexes reconstituted in vitro using unlabeled spleen actin and several fluorescent actin analogs. Apparent dissociation constants (K_d) were measured under low salt conditions with sedimentation equilibrium as described in Materials and Methods. Actin labeled while complexed with profilin had an ~10-fold lower affinity for profilin than did unlabeled spleen actin, but a 10-fold greater affinity for profilin than fluorescent actin analogs labeled at cys-374.

The DNase I binding site on actin has been mapped to a site on the surface of the actin molecule opposite to the side where profilin binds (Kabsch and Vandekerckhove, 1992). The binding site of this endonuclease is also important for actin–actin interactions (Kabsch and Vandekerckhove, 1992). We therefore tested whether our new actin labeling method produced an analog with a decreased capacity to inhibit DNase I since we prepared an actin molecule labeled at a site other than cys-374. When unlabeled actin or actin analogs were sedimented alone in the centrifugation experiments described above, the average fraction remaining in the top 40% of the sample of all of the samples as determined by DNase

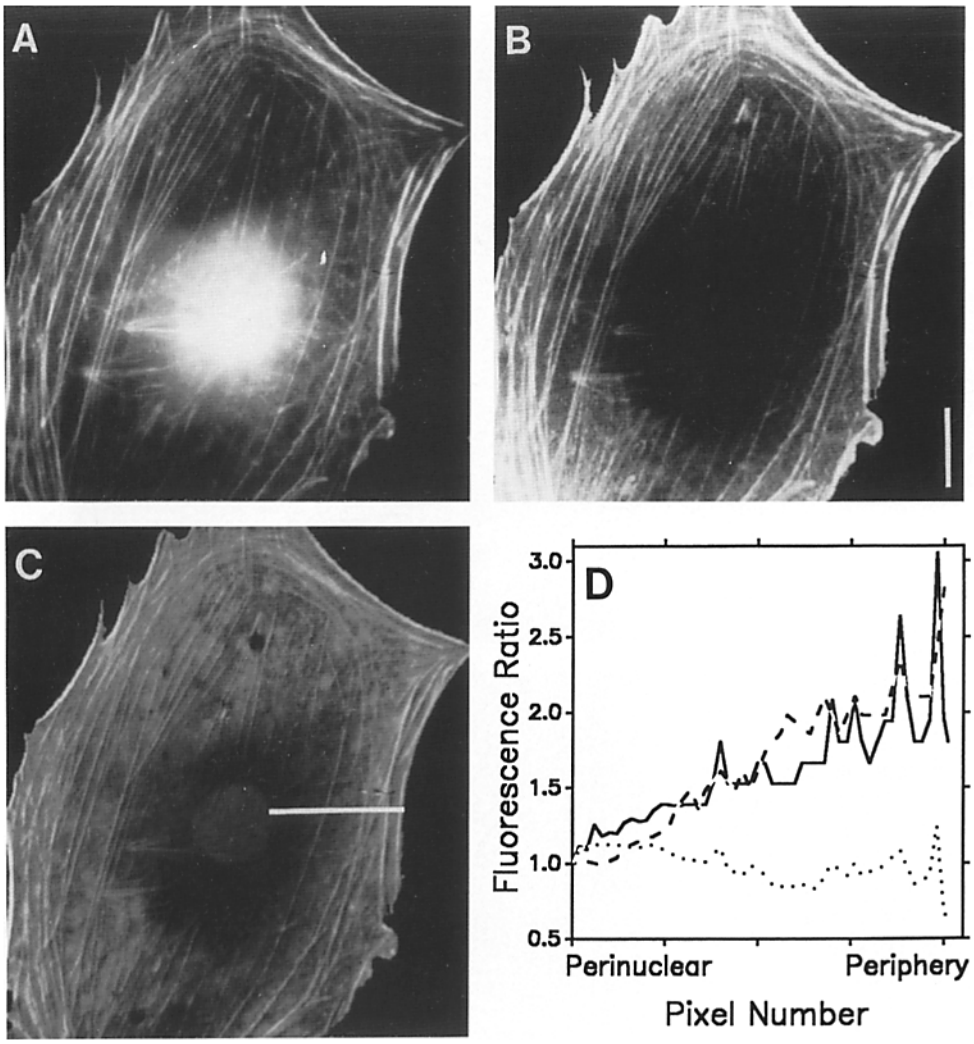

Figure 3. Fluorescent analogs of actin with an increased affinity for profilin exhibited a gradient of filament density relative to cell volume in serum-deprived cells. (*A*) Fluorescence image of sAmF-actin distribution in the cell depicted in Fig. 1. (*B*) Ratio image of sAmF-actin/volume marker (*A*/Fig. 1 *C*). (*C*) Ratio image of sAmF-actin/mAcR-actin (*A*/Fig. 1 *B*). The actin analog with the highest affinity for profilin (sAmF-actin) was concentrated in the peripheral regions of the cell, including stress fibers, relative to mAcR-actin in the same cell. (*D*) Fluorescence ratio values for the scan line depicted in *C*. Ratio values were normalized to one at the border between cell nucleus and perinuclear regions. Actin with an enhanced affinity for profilin (sAmF-actin) showed a gradient of filament density relative to a cell volume marker (*solid line*, data from *B*) and mAcR-actin (*dashed line*, data from *C*). However, cys-374–modified actin did not exhibit a gradient of filament density relative to cell volume (*dotted line*, data from Fig. 1 *D*). Bar, 10 μm.

I inhibition was 0.416 ± 0.036 (n = 12). The average fraction remaining of all of the actin analogs combined was 0.384 ± 0.036 (n = 10) as determined by spectrofluorometry. The two averages did not differ significantly ($p < 0.05$). Because the fraction of the actin remaining in the top 40% of each tube was the same using the two different measurements, the new actin analogs (sAmR-actin and sAmF-actin) and cys-374-labeled analogs (sAcF-actin, mAcF-actin, and mAcR-actin) inhibited DNase I to the same extent as did unlabeled spleen or muscle actin. Therefore, the new actin analogs exhibited greater affinity for profilin while maintaining the ability to bind to another class of actin-monomer-binding protein.

The New Actin Analog Exhibited a Gradient of Filament Density Relative to Cell Volume and a Gradient of Filament Assembly Relative to Cys-374–labeled Actin in Living Cells

In addition to a dextran volume marker and cys-374–labeled actin, the cell depicted in Fig. 1 was also microinjected with the actin analog having the higher affinity for profilin (sAmF-actin). The new actin analog distributed into stress fibers (Fig. 3 *A*) and showed a gradient of filament density relative to cell volume (Fig. 3, *B* and *D*, *solid line*), consistent with our original prediction. When the distribution of sAmF-actin and the cys-374–labeled actin (mAcR-actin) were directly compared by ratio imaging (Fig. 3, *C* and *D*, *dashed line*), we found that sAmF-actin was more concentrated in peripheral actin bundles (stress fibers) and less concentrated in the perinuclear region relative to mAcR-actin. This is consistent with a biased assembly of actin at the peripheral cytoplasm–membrane interface where profilin is most likely to release assembly-competent actin for incorporation into the cytoskeleton (Stossel, 1989).

The Translational Mobility of Actin Analogs in Living Cells is a Complex Summation of the Mobilities of a Wide Range of Actin Species

The striking difference in incorporation into the actin-based cytoskeleton between actin analogs due to their affinity for profilin (Fig. 3 *C*) led us to predict that the mobile fraction of the two actin analogs, based on fluorescence photobleaching recovery (FPR)[1] measurements, would show a similar

1. *Abbreviations used in this paper*: FPR, fluorescence photobleaching recovery; 3-D, three-dimensional.

Table I. The Translational Mobility of Two Fluorescent Actin Analogs in Serum-deprived Cells

Actin	Mobile fraction (%)*		M_{cyto}*
	Perinuclear	Periphery	$cm^2/s \times 10^{-8}$
mAcR	82 ± 3 (20)	66 ± 5 (13)	3.8 ± 0.85 (10)
sAmR	73 ± 4 (24)	52 ± 4 (12)	5.6 ± 1.1 (10)

* The average (± SEM) mobile fraction and cytoplasmic mobility (M_{cyto}) of two actin analogs were measured in living cells at 37°C using the fluorescence photobleaching recovery method described by Luby-Phelps et al. (1985). Numbers in parentheses indicate the number of determinations made in each case.

dependence on profilin binding. We found, however, that both actin analogs exhibited an immobile fraction in the range of 20–50% indicating that they incorporated into the actin-based cytoskeleton to some extent regardless of their affinity for profilin or location within the cytoplasm (Table I). While the mobile fraction of sAmR-actin and mAcR-actin in the periphery of cells was less than their respective mobilities in the perinuclear region ($p < 0.01$), the mobile fraction of sAmR-actin was not significantly different from mAcR-actin in either the periphery ($p > 0.025$) or the perinuclear region ($p > 0.05$) of serum-deprived cells. These results are consistent with earlier fluorescence photobleaching recovery studies showing that the translational mobility is similar for other fluorescent analogs of actin in living cells (Kreis et al., 1982; Luby-Phelps et al., 1985; Amato and Taylor, 1986). In addition, the FPR results demonstrate that the mobility of both types of actin analogs are lower in the periphery compared with the perinuclear region, consistent with more assembly in the periphery. However, since FPR measurements of mobility are directly proportional to the hydrodynamic radius of the labeled macromolecule, it is difficult to differentiate between actin monomers, actin multimers and actin complexed with actin-binding proteins. Therefore, FPR should not be used to interpret the subtleties of the distribution of the whole range of actin species.

Three-dimensional Imaging of the New Analog in Living Cells Revealed that Stress Fibers Were Localized in the Cortical Cytoplasm

Our results using fluorescence ratio imaging and fluorescence photobleaching recovery indicated that the mobile actin in the perinuclear cytoplasm was less assembled than the highly organized and significantly more immobile actin in the cell periphery. In some cells though, we observed that stress fibers coexisted with diffusely distributed actin in the perinuclear cytoplasm (Fig. 3 *A*) suggesting a heterogeneity of perinuclear actin assembly in the z-axis of the cell. We therefore performed three-dimensional (3-D) fluorescence microscopy on serum-deprived cells microinjected with sAmR-actin to map the distribution of actin. Serial sections through 40 serum-deprived cells were examined, and a rep-

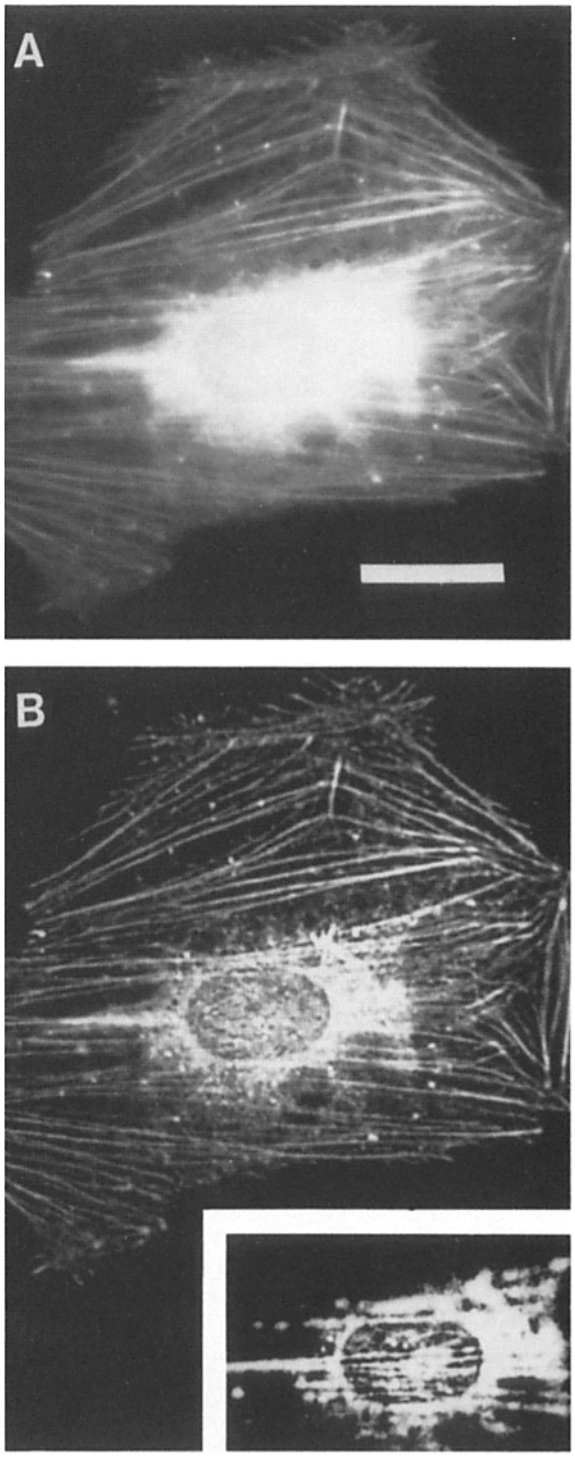

Figure 4. 3-D distribution of sAmR-actin in serum-deprived cells. We microinjected serum-deprived Swiss 3T3 fibroblasts with sAmR-actin and obtained a through-focus series of fluorescence images from each cell. We used a z-axis spacing of 0.32 μm between image planes. (*A*) The distribution of sAmR-actin as visualized by conventional fluorescence microscopy. The focal plane was close to the substratum (<0.5 μm above it). Cells exhibited an extensive array of peripheral stress fibers and diffusely distributed perinuclear actin characteristic of the quiescent, non-locomoting state of the cell. (*B*) Image A after deconvolution. The removal of most of the diffuse perinuclear fluorescence revealed stress fibers in the same optical section as the peripheral fibers. (*Inset*) A deconvoluted image from a plane lying near the top of the nuclear region, 2.53 μm above the plane shown in *B*. Peripheral stress fibers were dim in this plane and some of the bright perinuclear stress fibers were found to arch over the nucleus. Bar, 10 μm.

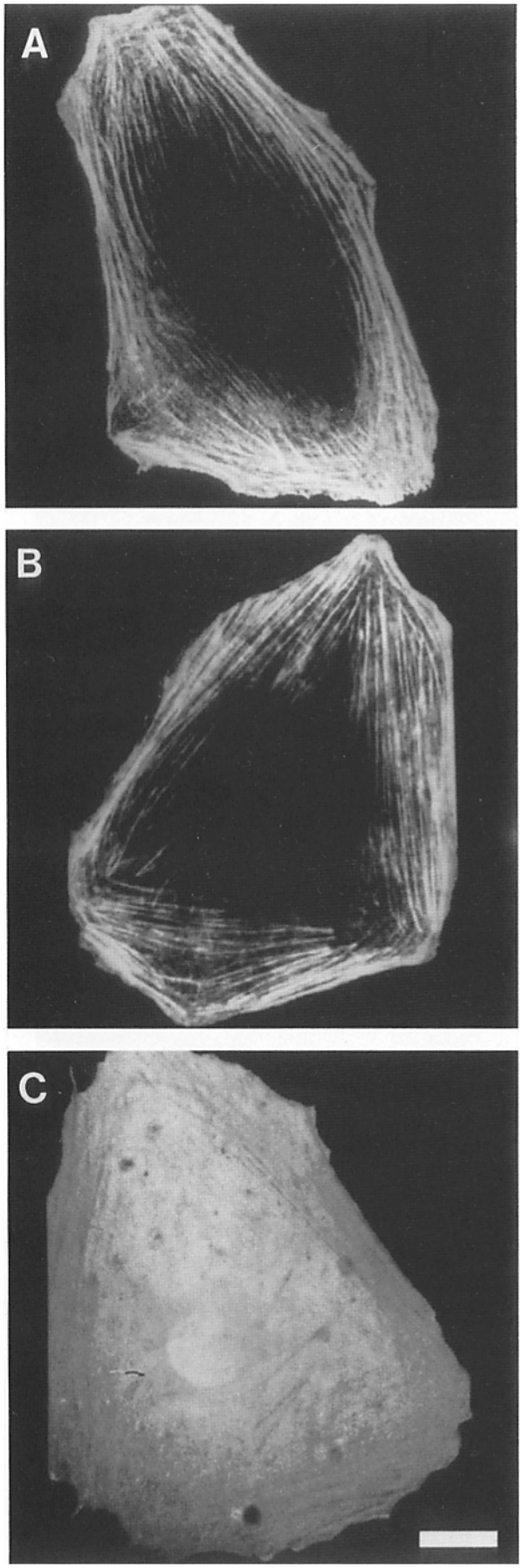

resentative cell is presented in Fig. 4. Stress fibers containing actin were consistently localized in the cortical cytoplasm. In the thin peripheral regions of the cell, there was no differentiation between dorsal and ventral cortical cytoplasm; only a single plane of stress fiber focus was detected (Fig. 4, *A* and *B*). In the thick perinuclear region, many cells exhibited ventral stress fibers (Fig. 4 *B*) or contained dorsal stress fibers that sometimes arched over the nucleus (Fig. 4 *B*, *inset*), or both. Hence, although some of the actin in the perinuclear cortical cytoplasm was incorporated into stress fibers, the highest mobility actin in the cell was found in the bulk perinuclear cytoplasm where constitutively transporting stress fibers are known to disassemble (Giuliano and Taylor, 1990). Furthermore, the 3-D distribution of actin described here was similar to the 3-D distribution of myosin II in serum-deprived cells where stress fibers containing myosin II are confined to the cortical cytoplasm (Kolega and Taylor, 1993).

The Biased Assembly of Actin Analogs in Living Cells Was Determined by the Site of Actin Labeling

Actin analogs with the highest affinity for profilin (sAmF-actin and sAmR-actin) were consistently more concentrated in peripheral cytoplasm and stress fibers relative to analogs with a lower affinity for profilin (mAcF-actin, mAcR-actin, and sAcF-actin) when their distributions were compared directly as in Figs. 3 *C* and 5, *A* and *B*. A control ratio image of two separate actin analogs, both with low affinities for profilin, demonstrated the lack of a gradient of concentration of the two analogs relative to each other (Fig. 5 *C*). The data further support the notion that biased assembly of profilin-competent actin analogs in the thin peripheral region of living cells depended only on the site of modification, not on the fluorescent dye used to label the actin or the tissue source of the actin.

Maintenance of a Gradient of Actin Assembly After Stimulation of Serum-deprived Cells Is Consistent with the Solation–Contraction Coupling Hypothesis

Upon addition of serum to serum-deprived cells, a transient increase in intracellular free calcium concentration occurs (Hahn et al., 1992), calmodulin is activated and binds to target proteins (Hahn et al., 1992; Gough and Taylor, 1993),

Figure 5. Actin analogs with the highest affinity for profilin were consistently more concentrated in the peripheral cytoplasm and stress fibers relative to analogs with a lower affinity for profilin. Serum-deprived cells, microinjected with two fluorescent analogs of actin and a labeled dextran volume marker, were subjected to ratio imaging as described in Fig. 1. (*A*) Ratio image of sAmR-actin/mAcF-actin. (*B*) Ratio image of sAmR-actin/sAcF-actin. (*C*) Ratio image of mAcR-actin/sAcF-actin. Cells containing actin analogs with different affinities for profilin consistently exhibited a relative gradient of concentration of the two with the high affinity analog concentrating into peripheral stress fibers (*A* and *B*). However, the source of actin (muscle or spleen) and the fluorescent probe (fluorescein or rhodamine) had no detectable effect on the results. Cells containing actin analogs with similar affinities for profilin displayed a relatively uniform distribution of the two actins (*C*). Bar, 10 μm.

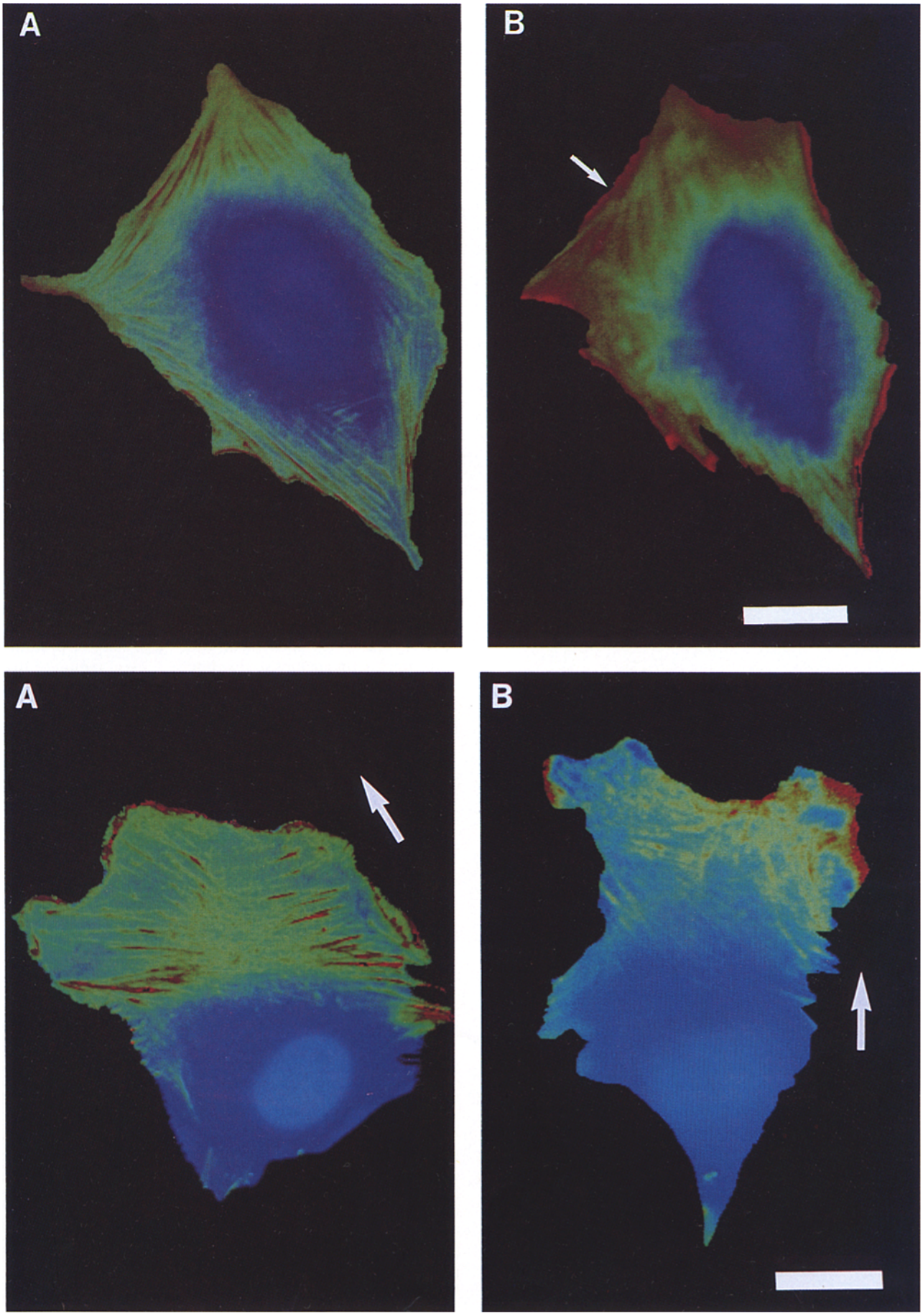
A
B
A
B

myosin II heavy and light chain phosphorylation increases causing many stress fibers to contract (Giuliano et al., 1992), and a contraction of the actin-based gel into the perinuclear region ensues (Giuliano and Taylor, 1990). The solation-contraction coupling hypothesis predicts that a contraction of the cytoplasmic gel would be accompanied by the release of monomeric gel components consistent with a self-destruct mechanism (Janson et al., 1991; Kolega et al., 1991; Janson and Taylor, 1993; Kolega and Taylor, 1993). We tested this prediction by measuring the gradient of actin assembly in serum-deprived cells before and after serum stimulation using ratio imaging (Fig. 6). Serum-deprived cells exhibited a gradient of filament density relative to cell volume maximal in the cell periphery (Fig. 6 *A*). One hour after serum-stimulation, video-enhanced contrast microscopy showed that much of the cytoplasmic gel had contracted into the perinuclear region as previously described (Giuliano and Taylor, 1990). Peripheral stress fibers were much less apparent, but actin filament density had increased in the periphery suggesting the stimulation of new actin assembly following contraction (Fig. 6 *B*). Although the cytoplasmic gel had initially been concentrated into the perinuclear region as detected by video-enhanced contrast microscopy, the actin filament density relative to the dextran volume marker in the perinuclear region did not increase. This is consistent with a transient contraction of the actin-based gel coupled with a concomitant decrease in the actin-based gel structure as predicted by the solation–contraction coupling hypothesis (Janson and Taylor, 1993). Note that serum stimulation caused a contraction of the stress fibers and less structured cytoplasmic gel meshwork (Giuliano and Taylor, 1990), and stimulated the movement of the cells beginning an hour after stimulation. Fig. 6 *B* shows the biased assembly of actin in the periphery, especially at the new leading edge (*arrow*).

Actin Exhibited a Gradient of Assembly That Was Maximal in the Leading Lamellae of Fibroblasts Undergoing Different Phases of the Wound Healing Response

The polarized assembly of actin and its interaction with myosin motors is believed to play a role in generating a directed contractile force for fibroblast locomotion (Fisher et al., 1988; Forscher and Smith, 1988; McKenna et al., 1989; Stossel, 1990; Hahn et al., 1992; Conrad et al., 1993; Gough and Taylor, 1993; Kolega and Taylor, 1993). We analyzed the gradients of actin assembly in highly polarized cells undergoing two phases of the wound-healing response. Fig. 7 *A* shows a gradient of actin assembly in a cell undergoing lamellar contraction, an early phase of the response (Conrad et al., 1993). The nearly ten-fold concentration of actin in transverse fibers and lamellipodia and its four-fold concentration elsewhere in the leading lamella relative to the volume marker in the perinuclear region was consistent with the assembly of actin initiated in the lamellipodia, formation of an actin-based cytoskeleton that transported rearward toward the tail, and a calcium-calmodulin–induced contraction that transiently concentrated actin in the fibers (Hahn et al., 1992; Conrad et al., 1993; Gough and Taylor, 1993). Cortical contraction has been proposed as a mechanism involved in detaching cells from neighbors, molding cell shape for free locomotion, and aiding in the delivery of subunits to the leading edge (DeBiasio et al., 1988; Hahn et al., 1992; Conrad et al., 1993; Gough and Taylor, 1993; Kolega and Taylor, 1993). Freely locomoting fibroblasts with few or no attachments to neighboring cells displayed a range of morphologies, yet consistently concentrated actin in their lamellipodia and lamellae relative to a volume indicator (Fig. 7 *B*). We interpreted this as a bias of actin assembly at the leading edge of migrating cells. Retracting tails also exhibited a gradient of filament density relative to a volume marker (Fig. 7 *B*). The perinuclear region appears to be the site of decreased actin assembly.

Discussion

Actin Is Concentrated by Incorporation into the Actin-based Cytoskeleton

Although the cytoplasm of Swiss 3T3 cells is broadly accessible to freely diffusible, labeled dextran molecules (Luby-Phelps et al., 1988), our results showed that actin analogs with a high affinity for profilin exhibited a gradient of filament density relative to dextran that was maximal in peripheral regions of the cytoplasm. In contrast to fixed, extracted, and fluorescent phalloidin-stained cells, ratio imaging of living cells allows us to account for the dynamic distribution of both the cytoskeletal-associated and the soluble forms of actin. By coinjecting cells with two different actin analogs and a fluorescent dextran to map the relative concentration of the actins with high spatial and temporal resolution, each

Figure 6. Serum-induced actin gel contraction and formation of new protrusions. (*A*) This pseudo-color ratio image (sAmR-actin/Cascade Blue dextran) depicts a gradient of filament density relative to cell volume similar to that shown for the serum-deprived cell described in Fig. 3 *B*. (*B*) Ratio image of the same cell measured one hour after stimulation with 10% serum. The pseudo-color look up tables for this pair of images were identical. The gradient of actin concentration became steeper following the serum-induced condensation of cytoplasmic material into the perinuclear region. Apparently, actin subunits were released after contraction and they became available for assembly in the newly polarized cell. Serum stimulation also initiated the polarization of the cell and the formation of a new leading edge with an increased concentration of actin in the new lamellipodia (*B, arrow*). Bar, 10 μm.

Figure 7. The polarization of actin filament density relative to cell volume occurs in cells undergoing different phases of the wound healing response. (*A*) The ratio of actin/volume marker indicated that actin was concentrated relative to the soluble dextran in the leading lamellae of the 20 cells observed undergoing the lamellar contraction phase of wound healing. The warmer red colors signify a ten-fold increase in the ratio values over the deepest blue color and a twofold increase over yellow-green colors. (*B*) Ratio image of a freely locomoting fibroblast generated using a modified wound healing protocol that minimized cell contacts. The ratio values indicated that filament density in the leading lamellae was generally twofold greater than in the perinuclear tail region. Actin incorporation into fibers resulted in ratio values four times those found in the perinuclear region. Bar, 10 μm.

cell became a complete experiment. This precluded the need to compare the statistical distribution of many actin analogs in a large number of separate and heterogeneous cells.

The highest density of actin filaments relative to cell volume was consistently found in cortical stress fibers. Thus, the concentration of actin molecules that results from biased filament assembly in the periphery of cells where surface/volume is maximal, followed by further concentration during bundling into fibers is consistent with our operational definition of actin assembly as described by ratio imaging (see Materials and Methods). We therefore interpreted the biased increase in filament density in the peripheral cytoplasm and stress fibers of serum-deprived cells as well as in the leading edge of locomoting cells as being a consequence of localized actin assembly and its incorporation into higher order actin-based structures. This is also consistent with our previous observation that stress fibers constitutively assemble in the thin peripheral regions of serum-deprived cells (Giuliano and Taylor, 1990) and at the leading edge of locomoting cells (Conrad et al., 1993).

Fluorescent phalloidin staining of fixed and extracted serum-deprived cells indicates that stress fibers can exist in the perinuclear region (Kolega et al., 1994). When visualized in living cells using fluorescent analogs of actin, perinuclear stress fibers are often obscured by the diffuse fluorescence from apparently less structured, labeled actin in the bulk cytoplasm. Three-dimensional fluorescence data, obtained here using a fluorescent actin analog and obtained elsewhere using a fluorescent analog of myosin II (Kolega and Taylor, 1993), show that some cortical fibers are maintained above and below the nucleus, but the highest density of fibers is found in the cell periphery where the volume of non-cortical cytoplasm is minimal. The low actin filament density in the perinuclear region of the cell relative to the volume marker was consistent with photobleaching measurements made through the entire thickness of the cell, and suggested that this was the location of the most mobile and therefore least cytoskeletally associated actin in the cell. This was also consistent with our previous observation that stress fibers constitutively disassemble in the perinuclear region of serum-deprived (Giuliano et al., 1990) and locomoting cells (Kolega and Taylor, 1993).

Interaction with Monomer Binding Proteins such as Profilin Is Important for the Biased Incorporation of Actin into the Cytoskeleton

In preparing our new actin analog the starting material was a high affinity profilactin complex isolated from bovine spleen (Carlsson et al., 1977). This complex, with a dissociation constant of <0.02 μM in Mg^{2+} (Katakami et al., 1992) and no detectable nucleotide (Carlsson et al., 1977; Lindberg et al., 1988), is difficult to reconstitute in vitro (Katakami et al., 1992). The original isolation of this high affinity profilactin complex prompted the still valid possibility that this physiologically derived form of profilactin acts as a reservoir of actin monomers in cells (Carlsson et al., 1977). Sanders and Wang (1990) found that monomer-binding proteins are likely to regulate the incorporation of actin into the cytoskeleton of living cells. Furthermore, microinjection of profilactin into cells induces the assembly of actin (Cao et al., 1992). Profilin has also been suggested to be concentrated in the lamellipodia of locomotory cells (Buß et al., 1992) where actin assembly has been detected (Wang, 1985; Fisher et al., 1988; Forscher and Smith, 1988; Theriot and Mitchison, 1992), although no ratio imaging measurements were made to normalize for optical pathlength. This recent evidence suggests that profilactin complexes do not necessarily act as a storage form of actin monomers.

Our live cell ratio imaging experiments using actin analogs with different affinities for profilin suggest that exchange of subunits with the actin-based cytoskeleton is enhanced when actin interacts with profilin or other actin binding proteins whose activity requires an unmodified actin cys-374 residue. Our photobleaching measurements did not detect a significant difference in the mobile fraction of two actin analogs whose affinity for profilin differed by an order of magnitude. The mobile fraction of actin within the cell has many components including actin monomers and oligomers, profilactin complexes, and actin monomers interacting with other soluble actin-binding proteins, thus making it difficult to resolve the exchange of actin between these pools. Likewise, photobleaching measurements would not be expected to differentiate between highly ordered states of F-actin in living cells (i.e., a loose meshwork of actin filaments versus actin incorporated into large stress fibers). On the other hand, ratio imaging detected differences between the cytoskeletal incorporation of actin analogs. Although the low profilin affinity, cys-374-modified actin analogs appeared to qualitatively yield similar results as the high profilin affinity actin analogs, some of the earlier quantitative studies of polarized actin dynamics should be re-addressed (Luby-Phelps et al., 1985; Wang, 1985; Theriot and Mitchison, 1992).

How Is a Gradient of Actin Assembly Maintained in Serum-deprived Cells?

We view the constitutive formation, transport, and disassembly of stress fibers in serum-deprived cells as an excellent opportunity to study the dynamics of actin and myosin II assembly–disassembly in living cells without the complications of whole cell movement and transient changes in pH and pCa (Giuliano et al., 1990, 1992; Kolega and Taylor, 1991, 1993; Kolega et al., 1991). The gradients of actin and myosin II (Kolega and Taylor, 1993) assembly that we observe in these cells must therefore be maintained under conditions of low intracellular free Ca^{2+} (McNeil and Taylor, 1987; Byron and Villereal, 1989; Tucker and Fay, 1990), minimal levels of Ca^{2+} activation (Hahn et al., 1992; Gough and Taylor, 1993), low and constant cytoplasmic pH (Bright et al., 1987), and partial phosphorylation of myosin II (Giuliano et al., 1992).

The gradient of actin assembly we observed appears to be more subtle than the gradient of myosin II assembly in the same cells because myosin II disassembles extensively into 10S particles in the perinuclear region (Kolega and Taylor, 1993) while, as we have shown here, actin maintains a cytoskeletally associated component in the same region. We previously showed that restricting the length of actin filaments in stress fibers without a change in the phosphorylation state of the myosin II associated with the fibers causes them to contract (Kolega et al., 1991; Giuliano et al., 1992). On the other hand, dephosphorylation and disassembly of myosin II without a change in the assembly state of actin causes stress fibers to splay apart without shortening (Kolega and Taylor, 1993), suggesting that actin filament disassembly

in these cells is coupled to the dephosphorylation and disassembly of myosin II.

Several actin binding proteins including profilin (Lassing and Lindberg, 1988), actin depolymerizing factor or destrin (Yonezawa et al., 1990), α-actinin (Fukami et al., 1992), gelsolin (Janmey and Stossel, 1989), and myosin I (Adams and Pollard, 1989) interact with phosphoinositides sequestered in membranes. This interaction could regulate the activity of these proteins near the membrane-cytoplasm interface, thus leading to a polarization of actin assembly that favors cortical polymerization. This is evident in the peripheral region of serum-deprived cells where the cortical cytoskeleton dominates over the non-cortical cytoplasm.

To dissect the regulation of gradient formation and to determine whether or not actin filaments disassemble completely to the monomer state we need to resolve the dynamic distribution of actin monomers and oligomers, actin complexed with monomer-binding proteins, and actin incorporated into the actin-based cytoskeleton. The fluorescence photobleaching experiments we describe here do not allow us to distinguish among the "soluble" forms of actin in the cell but steady state fluorescence anisotropy microscopy used in conjunction with carefully designed fluorescent analogs (Gough and Taylor, 1993) should allow us to map both the states of unassembled actin in living cells and the compartmentalization of actin-monomer binding proteins including profilin (Hartwig et al., 1989), actin depolymerizing factor (Hayden et al., 1993), and thymosin β4 (Goldschmidt-Clermont et al., 1992).

The Coordination of Actin Assembly and Myosin II Motor Activity during Fibroblast Locomotion

The existence of a gradient of actin and myosin II assembly, high at the front and low in the perinuclear region of migrating cells, can be explained as part of the cortical flow and solation–contraction coupling events that are believed to play a role in native cell locomotion (Taylor and Fechheimer, 1982; Bray and White, 1988; Conrad et al., 1993; Janson an Taylor, 1993; Kolega and Taylor, 1993). In addition to gradients of macromolecular assembly, migrating fibroblasts exhibit gradients of free calcium, calcium binding to calmodulin and calmodulin binding to target proteins, minimal at the leading edge and maximal in the posterior of the cells (Hahn et al., 1992; Gough and Taylor, 1993).

Our model of the roles that actin and myosin II play during "wild-type" fibroblast locomotion involves the precise regulation of the state of actin assembly and its interaction with myosin II to form a contractile gel (Fig. 8). It is predicted that short actin filaments will exist at the completion of the contraction in the perinuclear region in the tail due to the activity of gelsolin and other proteins that restrict the length of actin in a calcium-dependent manner. This would create a local elevation of actin monomer concentration. Profilactin, gelsolin–actin, and complexes of other actin–monomer-binding proteins may form with a bias in the perinuclear region in the posterior and then be transported or diffuse to the leading edge, or both, while continually exchanging actin subunits with the established cytoskeleton. Our data are consistent with a biased release of assembly competent actin, possibly by interacting with phosphoinositides, at the membrane–cytoplasm interface followed by net actin polymerization at the site of release. Therefore, a gradient of profilin

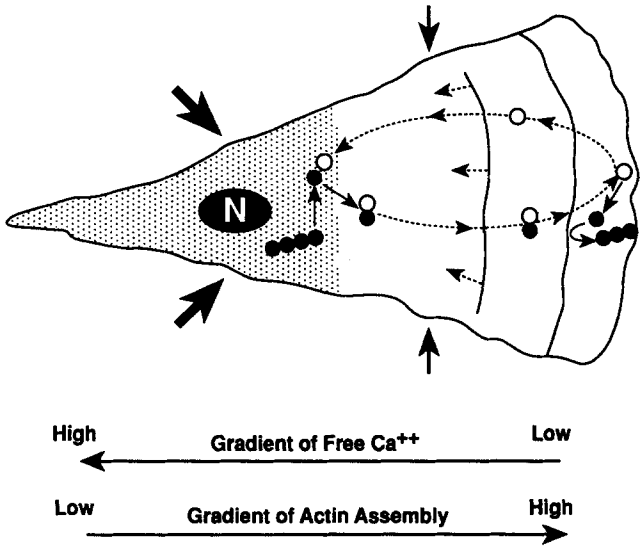

Figure 8. The role of actin assembly and myosin II motor activity during normal fibroblast locomotion. Actin (●) assembles with a bias at the leading edge with the aid of profilin and profilin-like molecules (○) (Wang, 1985; DeBiasio et al., 1988; Fisher et al., 1988; Forscher and Smith, 1988), forms transverse fibers at the base of lamellipodia, and transports rearward together with myosin II as part of the actin-based cortex (Conrad et al., 1993). Maximal contraction of the actin-myosin II cytoskeleton (*large arrows*) is initiated starting in the zone of elevated calcium (*shaded area*) by a combination of calcium activation of myosin light chain kinase and a decrease in the actin-gel structure through the action of calcium activation of severing proteins such as gelsolin (Hahn et al., 1992; Gough and Taylor, 1993). The cortical flow of the actin–myosin II (Bray and White, 1988), the initiation of contraction (Dunn, 1980), and the self-destruct nature of this cortical "corset" by solation–contraction coupling (*small arrows*) (Taylor and Fechheimer, 1982; Kolega et al., 1991) creates a cycle of biased assembly of actin at the front of the cell and disassembly toward the tail where the contraction is maximal. Myosin II exhibits a parallel gradient of assembly and a 3-D distribution similar to the distribution of actin described here (Kolega and Taylor, 1993).

concentration, low in the perinuclear region and high in lamellipodia would be consistent with but not required in our model system; the differential regulation of a uniform concentration of cytoplasmic profilin or profilin-like molecules, most likely driven by the proximity of phosphoinositides, would be enough to initiate a net release of assembly competent actin monomers in thin lamellipodia and a net binding of monomers in the perinuclear region. Profilin is markedly enriched in the lamellipodia of fixed cells (Buß et al., 1992), but the measurement of a cytoplasmic gradient of profilin concentration in living cells will require the ratio imaging techniques described here; such experiments are now underway in our laboratory.

A coupling of the events initiated by gradients in free Ca^{2+} concentration, calmodulin activation and target binding, and actin and myosin II assembly may, in turn, initiate a gradient of contraction of actin–myosin II in the cortex with a maximum in the tail (Hahn et al., 1992; Conrad et al., 1993; Gough and Taylor, 1993). These events would be predicted to control cell shape, optimize cell polarity, and possibly aid in the delivery of subunits to the leading edge

by creating a positive hydrostatic pressure. The increase in actin filament density in the tails of locomoting cells is due to the retraction fibers that would be predicted to contract due to the elevated calcium (Hahn et al., 1992) and calmodulin binding to targets (Gough and Taylor, 1993).

The complete mechanism of fibroblast locomotion probably involves a combination of distinct mechanisms coupled in time and space. The biased assembly of actin at the leading edge of migrating cells may also be important for other possible mechanisms involved in cell locomotion including: (*a*) motor activity of myosin I (Fukui et al., 1989; Pollard et al., 1991; Yonemura and Pollard, 1992; Conrad et al., 1993); (*b*) gel expansion (Oster and Perelson, 1987; Stossel, 1990; Condeelis, 1992); (*c*) osmotic pressure (Oster and Perelson, 1987; Stossel, 1990); (*d*) nucleation-release (Theriot and Mitchison, 1992); and (*e*) thermal fluctuations (Peskin et al., 1993). Additional mechanisms must be tested by mapping the distribution and activity of the major proteins and regulating processes. Using the living cell as a "microcuvette" will be an important complement to the tools of biochemistry, molecular biology, and genetics (Taylor et al., 1992).

We thank Charlotte Bartosh for maintaining the cultured cells for these experiments and Dr. Peter Berget for the use of his tabletop ultracentrifuge. We are also indebted to Drs. Kevin Burton, Greg Fisher, John Kolega, Jung Park, and Penny Post for critically reading the manuscript.

This research was supported in part by National Science Foundation Science and Technology Center grant DIR-8920118, award 2044A from the Council for Tobacco Research-U.S.A., and National Institutes of Health grant AR32461.

Received for publication 3 May 1993 and in revised form 4 January 1994.

References

Adams, R. J., and T. D. Pollard. 1989. Binding of myosin I to membrane lipids. *Nature (Lond.).* 340:565–568.

Amato, P. A., and D. L. Taylor. 1986. Probing the mechanism of incorporation of fluorescently labeled actin into stress fibers. *J. Cell Biol.* 102:1074–1084.

Amato, P. A., E. R. Unanue, and D. L. Taylor. 1983. Distribution of actin in spreading macrophages: A comparative study on living and fixed cells. *J. Cell Biol.* 96:750–761.

Aspenstrom, P., C. E. Schutt, U. Lindberg, and R. Karlsson. 1993. Mutations in β-actin: influence on polymer formation and on interactions with myosin and profilin. *FEBS (Fed. Eur. Biochem. Soc.) Lett.* 329:163–170.

Bray, D., and J. G. White. 1988. Cortical flow in animal cells. *Science (Wash. DC).* 239:883–888.

Bright, G. R., G. W. Fisher, J. Rogowska, and D. L. Taylor. 1987. Fluorescence ratio imaging microscopy: temporal and spatial measurements of cytoplasmic pH. *J. Cell Biol.* 104:1019–1033.

Bright, G. R., J. E. Whitaker, R. P. Haugland, and D. L. Taylor. 1989. Heterogeneity of the changes in cytoplasmic pH upon serum stimulation of quiescent fibroblasts. *J. Cell. Physiol.* 141:410–419.

Buß, F., C. Temm-Grove, S. Henning, and B. M. Jockusch. 1992. Distribution of profilin in fibroblasts correlates with the presence of highly dynamic actin filaments. *Cell Motil. Cytoskeleton.* 22:51–61.

Byron, K. L., and M. L. Villereal. 1989. Mitogen-induced $[Ca^{2+}]_i$ changes in individual human fibroblasts. Image analysis reveals asynchronous responses which are characteristic for different mitogens. *J. Biol. Chem.* 264:18234–18239.

Cao, L. G., G. G. Babcock, P. A. Rubenstein, and Y. L. Wang. 1992. Effects of profilin and profilactin on actin structure and function in living cells. *J. Cell Biol.* 117:1023–1029.

Carlsson, L., L. E. Nystrom, I. Sundkvist, F. Markey, and U. Lindberg. 1977. Actin polymerizability is influenced by profilin, a low molecular weight protein in non-muscle cells. *J. Mol. Biol.* 115:465–483.

Clarke, R. G., and G. J. Howlett. 1979. Determination of the molecular weight of proteins in heterogeneous mixtures: Use of an air-driven ultracentrifuge for the analysis of protein–protein interactions. *Arch. Biochem. Biophys.* 195:235–242.

Condeelis, J. 1992. Are all pseudopods created equal? *Cell Motil. Cytoskeleton.* 22:1–6.

Conrad, P. A., K. A. Giuliano, G. Fisher, K. Collins, P. T. Matsudaira, and D. L. Taylor. 1993. Relative distribution of actin, myosin I, and myosin II during the wound healing response of fibroblasts. *J. Cell Biol.* 120:1381–1391.

DeBiasio, R. L., L. L. Wang, G. W. Fisher, and D. L. Taylor. 1988. The dynamic distribution of fluorescent analogues of actin and myosin in protrusions at the leading edge of migrating Swiss 3T3 fibroblasts. *J. Cell Biol.* 107:2631–2645.

Dunn, G. A. 1980. Mechanisms of fibroblast locomotion. *In* Cell Adhesion and Motility. A. S. G. Curtis, and J. D. Pitts, editors. Cambridge University Press, Cambridge. 409–423.

Fisher, G. W., P. A. Conrad, R. L. DeBiasio, and D. L. Taylor. 1988. Centripetal transport of cytoplasm, actin, and the cell surface in lamellipodia of fibroblasts. *Cell Motil. Cytoskeleton.* 11:235–247.

Forscher, P., and S. J. Smith. 1988. Actions of cytochalasins on the organization of actin filaments and microtubules in a neuronal growth cone. *J. Cell Biol.* 107:1505–1516.

Fukami, K., K. Furuhashi, M. Inagaki, T. Endo, S. Hatano, and T. Takenawa. 1992. Requirement of phosphatidylinositol 4,5-bisphosphate for α-actinin function. *Nature (Lond.).* 359:150–152.

Fukui, Y., T. J. Lynch, H. Brzeska, and E. D. Korn. 1989. Myosin I is located at the leading edges of locomoting *Dictyostelium* amoebae. *Nature (Lond.).* 341:328–331.

Giuliano, K. A., and D. L. Taylor. 1990. Formation, transport, contraction, and disassembly of stress fibers in fibroblasts. *Cell Motil. Cytoskeleton.* 16:14–21.

Giuliano, K. A., M. A. Nederlof, R. DeBiasio, F. Lanni, A. S. Waggoner, and D. L. Taylor. 1990. Multi-mode light microscopy. *In* Optical Microscopy for Biology. B. Herman and K. Jacobson, editors. Wiley-Liss, New York. 543–557.

Giuliano, K. A., J. Kolega, R. DeBiasio, and D. L. Taylor. 1992. Myosin II phosphorylation and the dynamics of stress fibers in serum-deprived and stimulated fibroblasts. *Mol. Biol. Cell.* 3:1037–1048.

Goldschmidt-Clermont, P. J., M. I. Furman, D. Wachsstock, D. Safer, V. T. Nachimas, and T. D. Pollard. 1992. The control of actin nucleotide exchange by thymosin β4 and profilin. A potential regulatory mechanism for actin polymerization in cells. *Mol. Biol. Cell.* 3:1015–1024.

Gough, A. H., and D. L. Taylor. 1993. Fluorescence anisotropy imaging microscopy maps calmodulin binding during cellular contraction and locomotion. *J. Cell Biol.* 121:1095–1107.

Hahn, K., R. DeBiasio, and D. L. Taylor. 1992. Patterns of elevated free calcium and calmodulin activation in living cells. *Nature (Lond.).* 359:736–738.

Hartwig, J. H., and D. J. Kwiatkowski. 1991. Actin-binding proteins. *Curr. Opin. Cell Biol.* 3:87–97.

Hartwig, J. H., K. A. Chambers, K. L. Hopcia, and D. J. Kwiatkowski. 1989. Association of profilin with filament-free regions of human leukocyte and platelet membranes and reversible membrane binding during platelet activation. *J. Cell Biol.* 109:1571–1579.

Hayden, S. M., P. S. Miller, A. Brauweiler, and J. R. Bamburg. 1993. Analysis of the interaction of actin depolymerizing factor with G- and F-actin. *Biochemistry.* 32:9994–10004.

Heacock, C. S., and J. R. Bamburg. 1983. The quantitation of G- and F-actin in cultured cells. *Anal. Biochem.* 135:22–36.

Heath, J. P., and B. F. Holifield. 1991. Cell locomotion: New research tests old ideas on membrane and cytoskeletal flow. *Cell Motil. Cytoskeleton.* 18:245–257.

Janmey, P. A., and T. P. Stossel. 1989. Gelsolin-polyphosphoinositide interaction. Full expression of gelsolin-inhibiting function by polyphosphoinositides in vesicular form and inactivation by dilution, aggregation, or masking of the inositol head group. *J. Biol. Chem.* 264:4825–4831.

Janson, L. W., and D. L. Taylor. 1993. In vitro models of tail contraction and cytoplasmic streaming in amoeboid cells. *J. Cell Biol.* 123:345–356.

Janson, L. W., J. Kolega, and D. L. Taylor. 1991. Modulation of contraction by gelation/solation in a reconstituted motile model. *J. Cell Biol.* 114:1005–1015.

Kabsch, W. and J. Vandekerckhove. 1992. Structure and function of actin. *Annu. Rev. Biophys. Biomol. Struct.* 21:49–76.

Katakami, Y., N. Katakami, P. A. Janmey, J. H. Hartwig, and T. P. Stossel. 1992. Isolation of the phosphatidyl 4-monophosphate dissociable high-affinity profilin-actin complex. *Biochim. Biophys. Acta.* 1122:123–135.

Kolega, J., and D. L. Taylor. 1991. Regulation of actin and myosin II dynamics in living cells. *Curr. Top. Membr.* 38:187–206.

Kolega, J., and D. L. Taylor. 1993. Gradients in the concentration and assembly of myosin II in living fibroblasts during locomotion and fiber transport. *Mol. Biol. Cell.* 4:819–836.

Kolega, J., L. W. Janson, and D. L. Taylor. 1991. The role of solation-contraction coupling in regulating stress fiber dynamics in nonmuscle cells. *J. Cell Biol.* 114:993–1003.

Kolega, J., M. A. Nederlof, and D. L. Taylor. 1994. Quantitation of cytoskeletal fibers in fluorescence images: stress fiber disassembly accompanies dephosphorylation of the regulatory light chains of myosin II. *BioImaging.* In press.

Kreis, T. E., B. Geiger, and J. Schlessinger. 1982. Mobility of microinjected rhodamine actin within living chicken gizzard cells determined by fluorescence photobleaching recovery. *Cell.* 29:835–845.

Larsson, H., and U. Lindberg. 1988. The effect of divalent cations on the interaction between calf spleen profilin and different actins. *Biochim. Biophys. Acta.* 953:95–105.

Lassing, I., and U. Lindberg. 1988. Specificity of the interaction between phosphatidylinositol 4,5-bisphosphate and the profilin:actin complex. *J. Cell. Biochem.* 37:255–267.

Lindberg, U., C. E. Schutt, E. Hellsten, A.-C. Tjader, and T. Hult. 1988. The use of poly(L-proline)-Sepharose in the isolation of profilin and profilactin complexes. *Biochim. Biophys. Acta.* 967:391–400.

Luby-Phelps, K., F. Lanni, and D. L. Taylor. 1985. Behavior of a fluorescent analogue of calmodulin in living 3T3 cells. *J. Cell Biol.* 101:1245–1256.

Luby-Phelps, K., F. Lanni, and D. L. Taylor. 1988. The submicroscopic properties of cytoplasm as a determinant of cellular function. *Annu. Rev. Biophys. Biophys. Chem.* 17:369–396.

Malm, B. 1984. Chemical modification of Cys-374 of actin interferes with the formation of the profilactin complex. *FEBS (Fed. Eur. Biochem. Soc.) Lett.* 173:399–402.

Malm, B., H. Larsson, and U. Lindberg. 1983. The profilin-actin complex: Further characterization of profilin and studies on the stability of the complex. *J. Mus. Res. Cell Motil.* 4:569–588.

McKenna, N. M., Y. Wang, and M. E. Konkel. 1989. Formation and movement of myosin-containing structures in living fibroblasts. *J. Cell Biol.* 109:1163–1172.

McNeil, P. L., and D. L. Taylor. 1987. Early cytoplasmic signals and cytoskeletal responses initiated by growth factors in cultured cells. *Cell. Membr.* 3:365–405.

Okabe, S., and N. Hirokawa. 1989. Incorporation and turnover of biotin-labeled actin microinjected into fibroblastic cells: An immunoelectron microscopic study. *J. Cell Biol.* 109:1581–1595.

Oster, G. F., and A. S. Perelson. 1987. The physics of cell motility. *J. Cell Sci.* 8 (Suppl.):35–54.

Pagliaro, L., and D. L. Taylor. 1988. Aldolase exists in both the fluid and solid phases of cytoplasm. *J. Cell Biol.* 107:981–991.

Pardee, J. D., and J. A. Spudich. 1982. Purification of muscle actin. *Methods Enzymol.* 85:164–181.

Peskin, C. S., G. M. Odell, and G. F. Oster. 1993. Cellular motions and thermal fluctuations: the Brownian ratchet. *Biophys. J.* 65:316–324.

Pollard, T. D., S. K. Doberstein, and H. G. Zot. 1991. Myosin-I. *Annu. Rev. Physiol.* 53:653–681.

Rozycki, M., C. E. Schutt, and U. Lindberg. 1991. Affinity chromatography-based purification of profilin:actin. *Methods Enzymol.* 196:100–118.

Sanders, M. C., and Y. Wang. 1990. Exogenous nucleation sites fail to induce detectable polymerization of actin in living cells. *J. Cell Biol.* 110:359–365.

Stossel, T. P. 1989. From signal to pseudopod. How cells control cytoplasmic actin assembly. *J. Biol. Chem.* 264:18261–18264.

Stossel, T. P. 1990. How cells crawl. *Am. Sci.* 78:408–423.

Symons, M. H., and T. J. Mitchison. 1991. Control of actin polymerization in live and permeabilized fibroblasts. *J. Cell Biol.* 114:503–513.

Taylor, D. L., and M. Fechheimer. 1982. Cytoplasmic structure and contractility: The solation-contraction coupling hypothesis. *Philos. Trans. R. Soc. Lond. B. Biol. Sci.* 299:185–197.

Taylor, D. L., and Y. L. Wang. 1978. Molecular cytochemistry: Incorporation of fluorescently labeled actin into cells. *Proc. Natl. Acad. Sci. USA.* 75: 857–861.

Taylor, D. L., M. A. Nederlof, F. Lanni, and A. S. Waggoner. 1992. The new vision of light microscopy. *Am. Sci.* 80:322–335.

Theriot, J. A., and T. J. Mitchison. 1991. Actin microfilament dynamics in locomoting cells. *Nature (Lond.).* 352:126–131.

Theriot, J. A., and T. J. Mitchison. 1992. Comparison of actin and cell surface dynamics in motile fibroblasts. *J. Cell Biol.* 118:367–377.

Tucker, R. W., and F. S. Fay. 1990. Distribution of intracellular free calcium in quiescent BALB/c 3T3 cells stimulated by platelet-derived growth factor. *Eur. J. Cell Biol.* 51:120–127.

Wang, Y. L. 1984. Reorganization of actin filament bundles in living fibroblasts. *J. Cell Biol.* 99:1478–1485.

Wang, Y. L. 1985. Exchange of actin subunits at the leading edge of living fibroblasts: Possible role of treadmilling. *J. Cell Biol.* 101:597–602.

Wang, Y. L., and D. L. Taylor. 1980. Preparation and characterization of a new molecular cytochemical probe: 5-Iodoacetamidofluorescein-labeled actin. *J. Histochem. Cytochem.* 28:1198–1206.

Yonemura, S., and T. D. Pollard. 1992. The localization of myosin I and myosin II in *Acanthamoeba* by fluorescence microscopy. *J. Cell Sci.* 102: 629–642.

Yonezawa, N., E. Nishida, K. Iida, I. Yahara, and H. Sakai. 1990. Inhibition of the interactions of cofilin, destrin, and deoxyribonuclease I with actin by phosphoinositides. *J. Biol. Chem.* 265:8382–8386.